Carbohydrate Polymers 117 (2015) 177–184

Contents lists available at ScienceDirect

Carbohydrate Polymers

journal homepage: www.elsevier.com/locate/carbpol

Plasticized chitosan/polyolefin films produced by extrusion

Marie Matet, Marie-Claude Heuzey*, Abdellah Ajji, Pierre Sarazin

Chemical Engineering, Research Center for High Performance Polymer and Composite Systems—CREPEC, Polytechnique Montréal, 2500 chemin de Polytechnique, Montreal, QC, Canada H3 T 1J4

ARTICLE INFO

Article history:
Received 16 June 2014
Received in revised form
11 September 2014
Accepted 16 September 2014
Available online 30 September 2014

Keywords:
Plasticized chitosan
Melt processing
Extrusion
Polymer blend

ABSTRACT

Plasticized chitosan and polyethylene blends were produced through a single-pass extrusion process. Using a twin-screw extruder, chitosan plasticization was achieved in the presence of an acetic acid solution and glycerol, and directly mixed with metallocene polyethylene, mPE, to produce a masterbatch. Different dilutions of the masterbatch (2, 5 and 10 wt% of plasticized chitosan), in the presence of ethylene vinyl acetate, EVA, were subsequently achieved in single screw film extrusion. Very small plasticized chitosan domains (number average diameter <5 μm) were visible in the polymeric matrix. The resulting films presented a brown color and increasing haze with chitosan plasticized content. Mechanical properties of the mPE films were affected by the presence of plasticized chitosan, but improvement was observed as a result of some compatibility between mPE and chitosan in the presence of EVA. Finally the incorporation of plasticized chitosan affected mPE water vapor permeability while oxygen permeability remained constant.

© 2014 Elsevier Ltd. All rights reserved.

1. Introduction

Environmental concerns have led plastic research towards the development of new materials based on natural polymers in order to decrease synthetic polymers consumption and impact on the environment. Bio-based materials such as starch, cellulose, protein-based plastics and chitosan have been studied for several years because of their good properties such as biocompatibility and biodegradability (Mekonnen, Mussone, Khalil, & Bressler, 2013). Development of bio-based plastics is also an ideal way to use waste from agriculture or industries such as agro-processing and fisheries. Since these bio-based materials frequently suffer from mechanical weaknesses, blending with another thermoplastic may be a way to increase the bio-content in polymers while producing plastics with good functional properties and economically viable.

Chitosan is the most important derivative of chitin and is obtained through its deacetylation. Chitin is a biopolymer found, for instance, in the cell wall of fungi or in the shell of arthropods such as crustaceans (e.g., crabs, shrimps or lobsters), and is the most abundant polysaccharide on earth after cellulose (Domard & Rinaudo, 1983; Roberts, 1992). Because of its natural origin, non-toxicity, biocompatibility, biodegradability and antibacterial activity, chitosan has become a particularly interesting and attractive biomaterial in the last decades (Ravi Kumar, 2000; Rinaudo, 2006). Chitosan can be used in several areas such as food industry (food coatings or edible films to improve food conservation using its antifungal, antibacterial and antimicrobial activity), waste water treatment (filtration due to metal capture by chelation), cosmetics and biomedical applications such as drug delivery systems owing to its wound healing properties, or artificial skin due to its efficiency against bacteria and viruses and structural characteristics (Kittur, Kumar, & Tharanathan, 1998; Ravi Kumar, 2000; Rinaudo, 2006).

Chitosan films are generally produced by solvent casting, i.e. by dilution of chitosan raw powder or flakes in an acidic aqueous solution, casting in thin layers followed by solvent evaporation (Balau, Lisa, Popa, Tura, & Melnig, 2004; Dutta, Tripathi, Mehrotra, & Dutta, 2009). Films prepared using this technique present high brittleness because of the frictional force between polymer chains, a limited surface area and low production yield (Leceta, Guerrero, & de la Caba, 2013; Srinivasa, Ramesh, & Tharanathan, 2007).

To overcome these drawbacks, chitosan films should ideally be prepared through a molten route via film extrusion (Correlo et al., 2005; Martínez-Camacho et al., 2013) or internal mixing followed by compression molding (Mir, Yasin, Halley, Siddiqi, & Nicholson, 2011; Zhang, He, Liu, & Qia, 2009) like in the case of traditional thermoplastic polymers. However similarly to cellulose, chitosan exhibits a degradation temperature below its melting point, therefore chitosan-based materials prepared in typical

* Corresponding author. Tel.: +1 514 340 4711x5930; fax: +1 514 340 4159.
E-mail addresses: marie.matet@polymtl.ca (M. Matet), marie-claude.heuzey@polymtl.ca (M.-C. Heuzey), abdellah.ajji@polymtl.ca (A. Ajji), pierre.sarazin@polymtl.ca (P. Sarazin).

http://dx.doi.org/10.1016/j.carbpol.2014.09.058
0144-8617/© 2014 Elsevier Ltd. All rights reserved.

polymer processing equipment incorporate solid chitosan particles in the form of powder or flakes. Those composite materials present a poor visual aspect (presence of large elliptical chitosan particles with dimensions of 40–300 μm in length and 15–30 μm in thickness (Martínez-Camacho et al., 2013)) and low mechanical properties (Martínez-Camacho et al., 2013; Mir et al., 2011; Zhang et al., 2009) due to incompatibility between chitosan which is hydrophilic and the hydrophobic polymer matrix.

Chitosan plasticization allows obtaining a deformable phase. Indeed, plasticization results in a lower glass transition temperature (Meng, Heuzey, & Carreau, 2014) by decreasing the number of intermolecular bonds between polymer chains (Sears & Darby, 1982), and can improve film flexibility and facilitate chitosan processing (Srinivasa et al., 2007; Suyatma, Tighzert, Copinet, & Coma, 2005). In addition, plasticization in the "molten" state can be achieved through thermo-mechanical kneading, and production of chitosan-based films using this technique may approach industrial fabrication conditions. Such a plasticization technique has been developed since the nineties to facilitate the processing of bio-based plastics such as thermoplastic starch (TPS) (Avérous, 2004), cellulose acetate (Quintana, Persenaire, Bonnaud, & Dubois, 2012), protein-based plastics (Hernandez-Izquierdo & Krochta, 2008), polyhydroxyalkanoates (PHAs) (Holmes, 1985) or poly(lactic acid) (PLA) (Garlotta, 2001). More recently, this technique that uses mechanical and thermal energy, has been adapted to chitosan in the presence of polyols and an acetic acid aqueous solution to achieve plasticization (Epure, Griffon, Pollet, & Avérous, 2011; Matet, Heuzey, Pollet, Ajji, & Avérous, 2013).

In our previous work, chitosan plasticization was performed through thermo-mechanical treatment in an internal mixer in the presence of water, acetic acid and glycerol, and the plasticized material was melt-blended with metallocene polyethylene (mPE) and ethylene vinyl acetate (EVA) (Matet, Heuzey, & Ajji, 2014). Our observations have however revealed that the resulting chitosan plasticization was only partial and that an ordered microstructure remained. In the present work, the thermo-mechanical treatment is improved by achieving for the first time an extrusion process in order to produce a chitosan-based film with a higher degree of chitosan plasticization. Indeed, the processing method can affect the outcome of plasticization since higher shear stresses were shown to allow a reduction of processing temperature and the water content required to achieve starch plasticization, as reported by Liu, Xie, Yu, Chen, and Li (2009). A one-step extrusion process was developed for starch plasticization by Favis, Rodriguez, and Ramsay (2003, 2005) ten years ago. This approach, applied to chitosan, may allow chitosan plasticization and its blend with a thermoplastic polymer in a single step. It should provide a better control of the thermal degradation of plasticized chitosan by reducing mixing time and hence contact time between the polymers at high temperature, and it should also improve the dispersion of the chitosan phase. In this work, chitosan is plasticized using a one-step extrusion process in the presence of glycerol and an acetic acid solution, and directly blended with metallocene polyethylene (mPE). This masterbatch is then diluted with mPE in the presence of ethylene-vinyl acetate (EVA), for compatibilization purposes, in order to prepare films with different chitosan content. Detailed characterization of the chitosan-based materials is provided, including morphology, optical, thermal, mechanical, and oxygen and water vapor barrier properties.

2. Materials and methods

2.1. Materials

Chitosan in powder form (grade ChitoClear®) was purchased from Primex (Iceland). Its degree of deacetylation (DDA) is 96%, its weight-average molecular weight is in the range 250–300 kDa and it contains 0.1 wt% ash residue (according to the manufacturer's specifications). Glacial acetic acid and glycerol, used for chitosan plasticization, were purchased from Sigma-Aldrich and used as received.

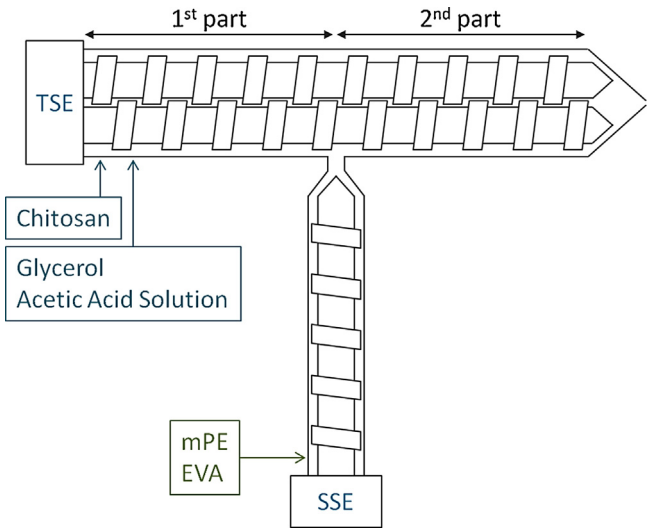

Fig. 1. Schematic representation of the one-step extrusion process.

Metallocene polyethylene (mPE) Affinity PL1880, with a melt flow index of 1 g/10 min at 190 °C (ASTM 1238), was purchased from Dow Chemicals (USA). The melting temperature is 99 °C, as determined by differential scanning calorimetry.

Ethylene vinyl acetate (EVA) Evatane 28-05, containing 28 wt% vinyl acetate, was obtained from Arkema (France). Its meting point is 72 °C and it presents a melt flow index of 5 g/10 min at 190 °C (ASTM 1238).

2.2. Sample preparation

The new procedure to prepare plasticized chitosan/polyolefin blend was based on the process developed by Favis et al. (2003, 2005). The specific screw profiles used were developed by Rodriguez-Gonzalez, Ramsay, and Favis (2003). The one-step extrusion process consisted in the use of a single-screw extruder (SSE) connected to a co-rotating twin-screw extruder (TSE) divided in 8 zones, as presented in Fig. 1. The SSE had a L/D = 26 with L = 495 mm (Brabender, Germany), while the TSE had a L/D = 28 with L = 960 mm (Leistritz, Germany). The SSE was used for the melting of the thermoplastic polymer (mPE) and its introduction in the TSE in zone 5. The TSE was divided in two functional parts: zones 1–4 were dedicated to chitosan feeding and plasticization and zones 5–8 to blending of plasticized chitosan and mPE.

Plasticized chitosan was prepared with 20 wt% chitosan, 60 wt% of a 3% v/v acetic acid solution and 20 wt% glycerol. Chitosan was fed in the first zone of the TSE at 0.75 kg/h. At the end of the first zone, the acetic acid solution and glycerol were fed together at 3 kg/h. Consequently, chitosan plasticization occurred in zones 2–4 of the TSE, at 105 °C and screw speed of 150 rpm. In the SSE, mPE was molten using a temperature range of 155 °C at the feeder to 180 °C at the connection with the TSE and screw speed of 110 rpm. The molten thermoplastic was introduced directly in zone 5 of the TSE at 4.5 kg/h. Then, plasticized chitosan and mPE were processed together in zones 5–8 at 130 °C and screw speed of 150 rpm. At the triple channel die exit, the extrudate was cooled in water and pelletized. A masterbatch containing 14 wt% of dry chitosan and 86 wt% of mPE was prepared, considering only the dry polymer

Table 1
Formulations of the films prepared.

Dry chitosan (wt%)	mPE (wt%)	EVA (wt%)
0	100	0
0	83	17
2	98	0
2	95	3
5	95	0
5	87.5	7.5
10	90	0
10	75	15

part. At this point, to prevent the presence of residual water or acid acetic, pellets were dried at 60 °C for 2 days under vacuum.

Different dilutions of the pellets previously prepared in masterbatch were achieved by film extrusion, using a single-screw extruder (Killion, USA) at 145 °C and 8.4 rpm. EVA was also added for compatibilization purposes with a constant EVA/chitosan ratio of 1.5. The produced films were cooled by calendaring rolls at 29 °C. Films without EVA were also prepared for comparison purposes. For the same reason, a film with only mPE and EVA was also prepared with the higher ratio mPE/EVA used (i.e. in the 10 wt% chitosan film, ratio of mPE/EVA was 5). The various formulations investigated are reported in Table 1.

2.3. Characterization

2.3.1. Scanning electron microscopy (SEM)

To visualize the films morphology, a scanning electron microscope JEOL JSM-840 (Japan) was used at 10 kV accelerating voltage. Several films were press molded together at 120 °C in order to prepare a thicker section then cross-sections of these samples were cut at −150 °C using a microtome equipped with a glass knife and coated with gold.

Semi-automatic image analysis was performed with the software SigmaScan Pro (USA) to quantify the dispersed plasticized chitosan domains surface area. For each film, the surface area of more than 200 domains was measured for different samples and at different magnifications.

2.3.2. Optical property characterization: Haze

UV-visible spectra of the films were obtained in accordance with the ASTM test method D1003. A Perkin Elmer Lambda 1050 spectrometer (USA) equipped with an integrating sphere was used. The total and diffuse transmittances were measured from 780 to 380 nm on several position of a film sample from each of two different batches of 25 × 25 mm^2 area. The haze was estimated as the ratio of diffuse to total transmittance.

2.3.3. Thermal behavior

2.3.3.1. Differential scanning calorimetry (DSC). DSC measurements were performed using a TA Instruments Q1000 (USA). Characteristic temperatures (crystallization and melting) were obtained from the second heating run at a rate of 10 °C/min from 25 °C to 150 °C, after a first run of heating up to 150 °C and cooling to 25 °C using the same rate, and under a nitrogen atmosphere. The weight of each sample was about 10 mg. Measurements were performed on processed films but also on neat polymers as received.

Crystallinity of the different samples (films and pellets as received) was calculated from the heat of fusion, determined by measuring the area of the melting peak and using this relationship: $X_c = \left(\Delta H_f / \Delta H_c\right) \times 100$, where X_c is the percentage of crystallinity, ΔH_f the fusion enthalpy of the sample and ΔH_c the fusion enthalpy of a perfectly crystalline polymer (280 J/g for polyethylene and 68 J/g for EVA). DSC measurements on chitosan alone did not reveal any crystallisation, glass transition or melting temperature.

2.3.3.2. Thermogravimetric analysis (TGA). A TA Instruments Q500 (USA) was used to determine the samples thermal degradation behavior. Temperature scans were performed from room temperature to 700 °C, using a heating rate of 10 °C/min under a nitrogen atmosphere. Each sample tested was less than 4 mg. Measurements were carried out on processed films but also on neat polymers as received.

2.3.4. Mechanical properties using uniaxial tensile testing

Tensile tests were performed on an Instron 3365 (USA). The tests were carried out at ambient temperature with films 2 cm wide and a gauge length of 5 cm. A constant stretching rate of 50 mm/min was applied. Mechanical properties were determined from the average of five measurements.

2.3.5. Barrier properties

Oxygen permeability was measured via a Mocon Ox-Tran Model 2/21 (USA) at ambient temperature and atmospheric pressure. The test cell used was a ST Module which can measure a transmission rate of 400 to 77,000 cm^3/m^2 day. The film tested (100 cm^2) was positioned between the two chambers. On one side, the chamber was full of oxygen, and on the other side the chamber was full of nitrogen. The system uses a coulometric sensor (Coulox®) to detect oxygen transmission from one chamber to the other one.

The permeability to water vapor was measured via a Mocon Aquatran Model 1 (USA) designed for measuring low water vapor transmission, from 0.5×10^{-3} to 15×10^{-3} cm^3/m^2 day. Tests were performed at ambient temperature and atmospheric pressure. Films tested were 5 cm^2 in surface area.

For all permeability tests, four different samples of two different batches were analyzed.

2.3.6. Porosity measurement

The liquid intrusion method was used to measure porosity in mPE films. Some small section of films (15 × 15 mm^2 area) were first weighed and then immersed in a solution of pure ethanol overnight. Films were removed from the solution and their surface was softly wiped in order to remove ethanol in excess. Then, samples filled with ethanol were weighed. This measurement was performed for three specimens.

Porosity was calculated using the following equation:

$$\text{Porosity}\ \ (\%) = \frac{\nu_{\text{EtOH}}}{\left(\nu_{\text{EtOH}} + \nu_{\text{mPE}}\right)} \times 100$$

where $\nu_{\text{mPE}} = m_{\text{dry}}/\rho_{\text{mPE}}$ is the volume of the mPE film with m_{dry} the mass of the dry film and ρ_{mPE} the mPE density (0.902 mg/mm^3), and $\nu_{\text{EtOH}} = \left(m_{\text{wet}} - m_{\text{dry}}\right)/\rho\text{EtOH}$ is the volume occupied by ethanol in the pores of the film with m_{wet} the mass of the wet film and ρ_{EtOH} the ethanol density (0.789 mg/mm^3).

Another technique was used to correlate results by comparing apparent and theoretical density. To calculate the apparent density, the width and length of the samples were measured using a digital caliper and thickness using a digital thickness gage. Then, porosity was evaluated using the following equation:

$$\text{Porosity}\ \ (\%) = \left(1 - \rho_{\text{app}}/\rho_{\text{mPE}}\right) \times 100$$

where ρ_{app} is sample mass divided by its volume.

3. Results and discussion

3.1. Microstructure

Fig. 2 presents SEM images of the different mPE films prepared with 2, 5 or 10 wt% of dry chitosan (complete formulation described in Table 1) and compatibilized using EVA. Some small plasticized chitosan domains are visible in the polymeric matrix

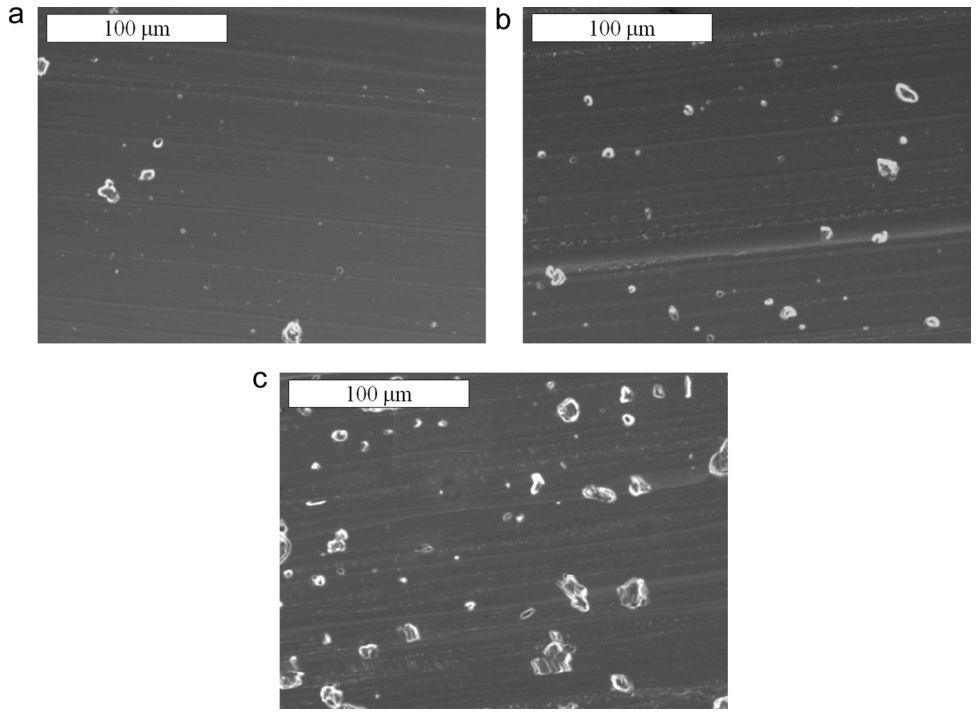

Fig. 2. SEM micrographs of different films compatibilized with EVA. (a) 2 wt% chitosan, (b) 5 wt% chitosan and (c) 10 wt% chitosan.

with no evidence of coalescence of chitosan domains, in agreement with previous studies (Martino, Pollet, & Avérous, 2011; Matet et al., 2014).

The size of the visible domains was measured and no influence of the chitosan content was noticed. Chitosan plasticized domains were more spherical after twin-screw extrusion than the internal mixing process (Matet et al., 2014). More than 55% of the plasticized chitosan domains showed a diameter lower than 5 μm, and more than 35% had a diameter between 5 and 10 μm. All chitosan domains measured were lower than 150 μm^2 in surface area. This value is smaller than the range previously observed for blends with similar formulation but prepared using an internal mixer (100 to 500 μm^2) (Matet et al., 2014). This may be explained by the larger shear rate and the presence of a higher elongational flow component encountered in twin-screw extrusion, in comparison with internal batch mixing. Indeed, using a rough approximation, internal mixer and twin-screw extruder have been modeled as a Couette geometry and the calculated shear rate (Marić & Macosko, 2001) was 90 s^{-1} in the internal mixer at 100 rpm rotor speed (Matet et al., 2014), and 270 s^{-1} in twin-screw extrusion at 150 rpm. Also, whatever the range of viscosity, it is has been shown that the breakage of the dispersed phase was easier in an elongational flow field (Favis & Therrien, 1991). This increase in shear rate and elongational flow should improve plasticization (Liu et al., 2009). However a few large particles (around 100–150 μm^2 in surface area) still present in small number indicate that chitosan plasticization was not completely achieved and could be improved further.

The size range of plasticized chitosan domains observed here is also smaller than chitosan particles in composite films prepared by twin-screw extrusion but without the plasticization step. In such cases, the morphology of the composite films showed that chitosan particles were about the same size than before processing. The size range of chitosan particles reported in this case was between 100 and 300 μm^2 (Bonilla et al., 2013; Correlo et al., 2005).

Finally, the size of the chitosan plasticized domains observed in the presence of EVA was the same as for films prepared without EVA (results not shown). Indeed, since plasticization occurred during the twin-screw extrusion step, the second pass performed in the single-screw extruder for masterbatch dilution and film extrusion did not allow reducing the size of the chitosan domains.

3.2. Optical properties: Haze

Even if the chitosan powder is originally yellowish, the films presented a brown color, more intense as the chitosan content increased as presented in Fig. 3. That is probably due to the Maillard reaction that can occur when the carbonyl group reacts with the amino group (Namiki, 1988). This reaction is accelerated in the presence of water and high temperature. The Maillard reaction can result in a brownish color (Tanaka et al., 1993).

Fig. 4 shows the haze value measured for the different films prepared. As expected, haze increased with the presence of chitosan. In comparison with the neat mPE, the addition of chitosan at 2, 5 and 10 wt% led to a multiplication by, respectively, 4.4, 15.5 and 22.1 of the haze value. On the other hand, the addition of EVA in the formulation of the films did not have a constant trend on haze. For 2 wt% chitosan, EVA led to an increase of 24% of the haze, whereas, for 5 wt% chitosan, it caused only a slight increase of 5%. Surprisingly, in the case of 10 wt% chitosan, the addition of EVA induced a decrease of 20% in haze. Indeed, when the EVA quantity increased in the films, their aspect was glossier and that could have influenced the haze value. This effect is not understood yet since no noticeable differences were observed in the size of the plasticized chitosan domains with and without EVA. However, lower mPE cristallinity (next section) in the presence of EVA may contribute to better optical properties.

3.3. Thermal properties

Characteristic temperatures (crystallisation and melting) and percentage of crystallinity obtained by DSC and TGA (degradation) are reported in Table 2. The first part of Table 2, shaded in grey, presents characteristic temperatures of the three polymers used as received. The second part of Table 2 presents characteristic

Fig. 3. Plasticized chitosan-based films for different chitosan content.

temperatures of samples prepared after the one-step extrusion process and film extrusion. The first derivative of the thermogravimetric curves showed a degradation in one stage for all the samples, excepted for the neat EVA who exhibited a thermal degradation in two stages. The maximum temperatures in the first derivative curves for one or two stages are reported in Table 2 as T_{dmax}, with the corresponding remaining weights.

Crystallisation and melting temperatures of the neat mPE film were respectively 86 and 100 °C, which is the same as the mPE as received. EVA presented lower characteristic temperatures: 50 and 72 °C, respectively, for crystallisation and melting temperatures.

As shown in Table 2, whatever the chitosan percentage present in the mPE/EVA films, characteristic temperatures remained constant.

It appears that mPE showed a higher crystallinity than EVA, while the mPE/EVA film exhibited an intermediate value of crystallinity. The crystallinity content did not decrease significantly after the addition of plasticized chitosan, but did in the combined presence of chitosan and EVA.

The $T_{98\%}$, $T_{50\%}$ and T_{dmax} values show that the mPE film degradation was faster after processing than the mPE pellets as-received, possibly due to the thermo-mechanical treatment, even though mPE is not recognized to be prone to this type of degradation. As-received EVA, a copolymer of ethylene and vinyl acetate, presented a thermal degradation in two steps indicated in Table 2 as 1st and 2nd for T_{dmax} and the corresponding weight.

Fig. 5 presents TGA curves for the different films prepared with plasticized chitosan, mPE and EVA. The chitosan content present in the film was evaluated from the residue obtained at the end of the TGA experiment, attributed only to chitosan. True chitosan content was estimated to be 1.2, 4.1 and 8.7 wt%, respectively, for the films with a nominal content of 2, 5 and 10 wt% of chitosan.

In the presence of chitosan, thermal degradation tended to be initiated earlier (decreased $T_{98\%}$) as the chitosan content increased. This result was predictable since chitosan alone showed a faster thermal degradation than mPE. However, the $T_{50\%}$ value was nearly, stable independently of the chitosan content in comparison with the mPE alone. This may indicate that the thermal degradation of chitosan was not dominant in the remaining part of the curve and could be attributed strictly to mPE.

In the thermal degradation of the different films was also slightly faster in the presence of EVA, which by itself showed a faster degradation than mPE (Table 2).

Table 2
Thermal properties measured by DSC and TGA for the neat polymers and the different films prepared.

Sample	DSC			TGA			
	T_c (°C)	T_m (°C)	X_c (%)	$T_{98\%}$ (°C)	$T_{50\%}$ (°C)	1st derivative	
						T_{dmax} (°C)	Weight (%)
mPE (as-received)	88	100	21	441	493	497	39
EVA (as-received)	50	72	17	329	478	366 (1st)488 (2nd)	88 (1st)31 (2nd)
Chitosan (as-received)	–	–	–	36	361	311	71
mPE	86	101	20	416	472	477	36
mPE + EVA	86	99	18	369	475	478	30
2 wt% Chitosan + mPE	86	101	19	371	472	477	35
2 wt% Chitosan + mPE + EVA	86	100	18	305	469	475	35
5 wt% Chitosan + mPE	86	100	18	194	470	476	34
5 wt% Chitosan + mPE + EVA	86	100	16	191	468	474	34
10 wt% Chitosan + mPE	86	100	18	160	469	475	34
10 wt% Chitosan + mPE + EVA	86	100	15	155	466	473	36

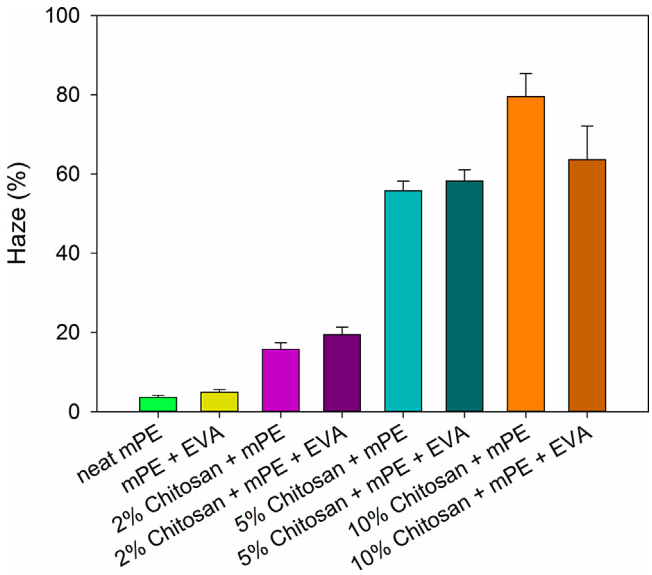

Fig. 4. Haze value for the different films prepared.

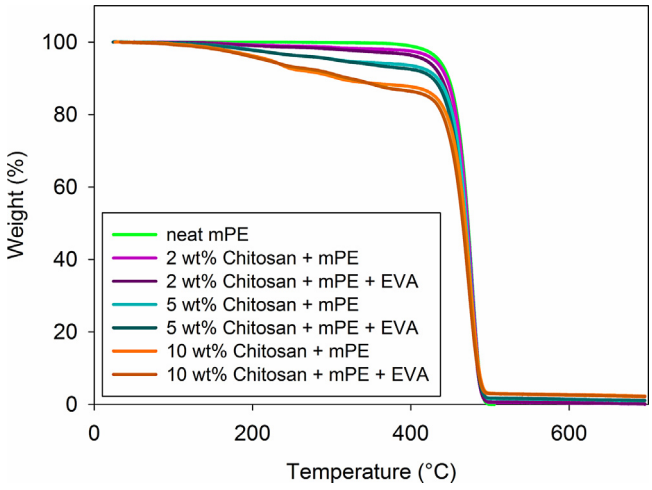

Fig. 5. TGA curves of plasticized chitosan/mPE and EVA films.

3.4. Mechanical properties

Fig. 6 shows typical stress–strain tensile curves and the average mechanical properties of neat mPE, mPE/EVA, plasticized chitosan/mPE, and plasticized chitosan/mPE/EVA films containing different chitosan contents.

Neat mPE presented a ductile behavior with an important plastic deformation. This behavior was somehow influenced by the presence of plasticized chitosan and EVA.

The elastic modulus of neat mPE was negatively affected by the addition of plasticized chitosan, and continued to decrease with the EVA addition, except for the 10 wt% chitosan film. Indeed, EVA itself exhibits a poor elastic modulus in comparison with mPE (Matet et al., 2014), in and had a negative influence on the behavior of the mPE/EVA film. On the other hand, the decrease of the elastic modulus in the presence of chitosan seems to indicate that chitosan did not act as a filler but as a second (or third) polymeric component in the film, which may confirm successful chitosan plasticization.

Tensile stress at yield decreased with plasticized chitosan, however, EVA had some influence (8% increase for 2 wt% and 5 wt% chitosan, and 13% increase for 10 wt% chitosan after the addition

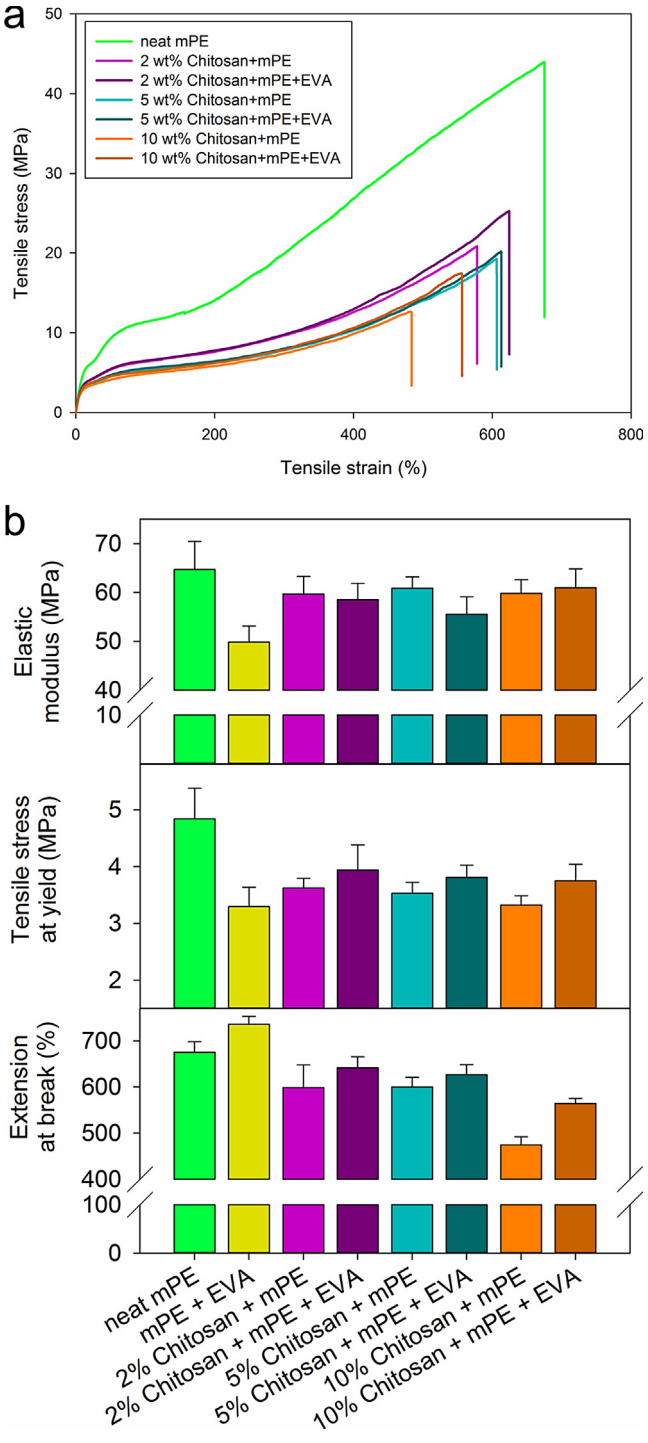

Fig. 6. Mechanical properties of neat mPE and various plasticized chitosan/mPE/EVA based films (a) Typical stress–strain curves, (b) tensile properties.

of EVA), showing that it partly played its role as a compatibilizer between mPE and plasticized chitosan.

Extension at break of mPE was also influenced by plasticized chitosan. Addition of 2, 5 and 10 wt% of chitosan led to a decrease in extension at break of 11, 11 and 30%, respectively. After compatibilization with EVA, the decrease in extension at break was less impacted by plasticized chitosan, the decrease was only 5, 7 and 16% for 2, 5 and 10 wt% of chitosan, respectively.

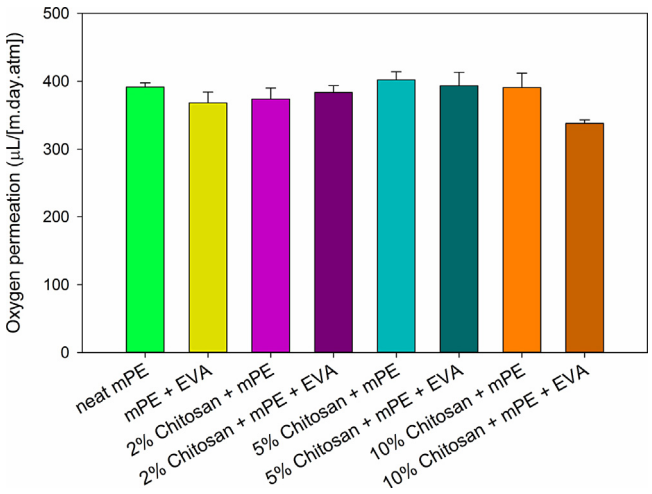

Fig. 7. Oxygen permeability of different films at ambient temperature and pressure.

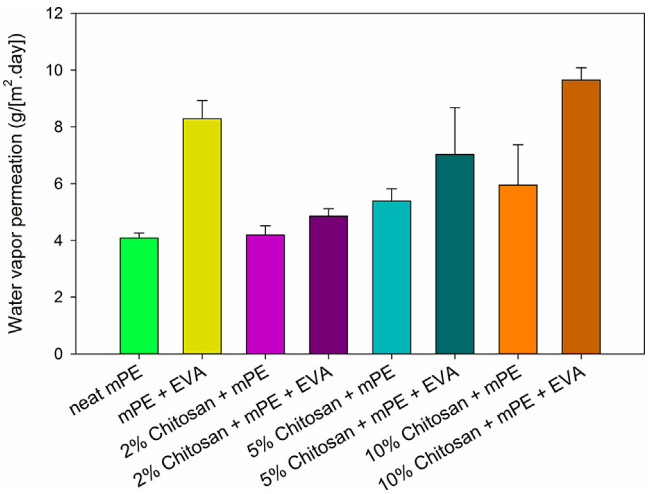

Fig. 8. Water vapor permeability of different films at 100%RH, 37.8 °C and ambient pressure.

3.5. Barrier properties

3.5.1. Oxygen permeability

Transport mechanisms for a gas through a polymeric film can be divided into three main stages: first, adsorption of the gas by the film at the interface with the ambient atmosphere; second, the gas diffusion inside and through the polymer film via a series of jumps from a free space to another, this step is the slowest; third, desorption and diffusion of the gas from the film interface to the ambient atmosphere (McKeen, 2012a). Depending on its own barrier properties and quality of the film, the addition of a second polymer or filler can increase or decrease the barrier properties of a polymeric film. Also, crystallinity of the film will have an impact on the quality of barrier properties: generally permeability decreases when the percentage of crystallinity increases (Flaconneche, Martin, & Klopffer, 2001). Fig. 7 presents the oxygen permeability measured for films of neat mPE, mPE and EVA, and the different films prepared with plasticized chitosan, mPE and EVA. The neat mPE film presented a high oxygen permeability (400 µL/[m day atm]), the same order of magnitude than low density polyethylene (225 µL/[m day atm] for PE with a density of 0.915 g/cm^3) (McKeen, 2012b), which is reasonable considering that the density of mPE Affinity PL1880G is 0.902 g/cm^3. The permeability was nearly unchanged after the addition of plasticized chitosan and EVA. Those results were not expected. Indeed, addition of chitosan or EVA should lead to an increase in oxygen permeability. Chitosan films alone prepared by solvent casting exhibit low oxygen barrier properties (7 µL/[m day atm]) (Leceta et al., 2013a), even lower than mPE or EVA (450 µL/[m day atm]) (McKeen, 2012a). Also, the glycerol present in the plasticization formulation may have an effect on permeability: it was shown that oxygen permeability increased in the presence of glycerol (Kurek et al., 2012; Leceta et al., 2013b). In addition, EVA enhances the polarity of polyethylene, leading to a loss of interaction between the polymer and non-polar oxygen, causing higher oxygen permeability. Besides, EVA has large vinyl acetate side groups, and, when mixed with mPE, the space between the polymer chains increases, resulting in more channels for oxygen transportation (Ali Dadfar, Alemzadeh, Reza Dadfar, & Vosoughi, 2011). In addition, a slight decrease in the percentage of crystallinity observed from DSC (Table 2) for the film with the highest content of plasticized chitosan and EVA and should have resulted in a higher permeability, contrary to what Fig. 7 shows. Two different approaches, namely the comparison of true and theoretical density and liquid intrusion method, were used to verify the possible presence of pores in the films that could control the oxygen permeability and rule out the effect of formulation. However the presence of pores was not evidenced by any of the characterization technique. Overall it is possible that the high oxygen permeability of neat mPE could not be worsened by the presence of plasticized chitosan and EVA.

3.5.2. Water vapor permeability (WVP)

Water vapor permeability (WVP) values are presented in Fig. 8 for films of neat mPE and the different films prepared with plasticized chitosan, mPE and EVA. The presence of chitosan clearly leads to an increase of the WVP value. That can be explain by the strong hydrophilic character of chitosan (Rinaudo, 2006) by opposition to the hydrophobic character of mPE. The transport of water molecules through the film could have been facilitated after the addition of plasticized chitosan. Also, since EVA is a copolymer with vinyl acetate groups, it would be more polar that mPE and would allow easier transport of water molecules through the film. Note that according to Table 1, the content of EVA varies according to the quantity of chitosan, except for sample mPE + EVA that contains nearly as much EVA than sample 10% chitosan + mPE + EVA. Therefore the combined effect of EVA and plasticized chitosan greatly increases the permeability of the films to water vapor.

4. Conclusions

In this work, polymeric films with 2, 5 and 10 wt% of plasticized chitosan were produced for the first time through an extrusion process. A twin screw extruder (TSE) allowed chitosan plasticization and its blending with molten mPE and EVA, fed in parallel by a single screw extrusion (SSE) connected to the TSE.

SEM images of the films showed plasticized chitosan domains more than 5 times smaller than the particles observed for films prepared by internal batch mixing in previous studies. Visual aspect and haze were affected by the addition of chitosan, the intensity of the brown color of the film and the haze increased with plasticized chitosan content. Characteristic temperatures of mPE (melting and crystallisation temperatures) remained constant independently of the chitosan quantity present in the film. Also, thermal degradation tended to be initiated earlier in the presence of chitosan and when its content increased. Mechanical properties were also affected by the presence of chitosan. However, a small content of plasticized chitosan (2 wt% of dry chitosan) did not have a strong effect on the elastic modulus and extension at break. Finally, oxygen

permeability was not affected by the addition of plasticized chitosan while water vapor permeability increased.

The presence of EVA could also help to enhance compatibilization between mPE and plasticized chitosan, as shown by the improvement of mechanical properties. Nevertheless, the films obtained after the addition of EVA did not demonstrate the same mechanical properties than mPE alone. We speculate that the overall microstructure and properties may be improved by using an EVA with higher vinyl acetate content. Furthermore, twin-screw extrusion for simultaneous masterbatch dilution and film production may allow obtaining a better blend of mPE, EVA and plasticized chitosan, along with films with better optical quality.

The extrusion process proposed here allows the preparation of plasticized chitosan-based materials on an industrial scale. The morphology of these films is finer than what was obtained in previous studies based on batch mixing, the mechanical properties of mPE are nearly unaffected and the visual aspect of the films remains acceptable. Nevertheless more studies remain to be achieved in order to improve further the material properties, both in terms of material formulation and processing conditions.

Acknowledgments

The authors acknowledge the NIPMMP (Network for Innovative Plastic Materials and Manufacturing Processes) of NSERC (Natural Sciences and Engineering Research Council of Canada) for the financial support of this work. The authors would like to thank Dr. Basil Favis and Aymen Ghouila of Cerestech Inc. for their help in the development of the one-step extrusion process. The authors also thank Guillaume Lessard at Polytechnique Montreal for his valuable assistance in film extrusion.

References

Ali Dadfar, S. M., Alemzadeh, I., Reza Dadfar, S. M., & Vosoughi, M. (2011). Studies on the oxygen barrier and mechanical properties of low density polyethylene/organoclay nanocomposite films in the presence of ethylene vinyl acetate copolymer as a new type of compatibilizer. *Materials & Design*, *32*(4), 1806–1813.

Avérous, L. (2004). Biodegradable multiphase systems based on plasticized starch: A review. *Polymer Reviews*, *44*(3), 231–274.

Balau, L., Lisa, G., Popa, M., Tura, V., & Melnig, V. (2004). Physico-chemical properties of chitosan films. *Central European Journal of Chemistry*, *2*(4), 638–647.

Bonilla, J., Fortunati, E., Vargas, M., Chiralt, A., & Kenny, J. M. (2013). Effects of chitosan on the physicochemical and antimicrobial properties of PLA films. *Journal of Food Engineering*, *119*(2), 236–243.

Correlo, V. M., Boesel, L. F., Bhattacharya, M., Mano, J. F., Neves, N. M., & Reis, R. L. (2005). Properties of melt processed chitosan and aliphatic polyester blends. *Materials Science and Engineering a-Structural Materials Properties Microstructure and Processing*, *403*(1–2), 57–68 [Article].

Domard, A., & Rinaudo, M. (1983). Preparation and characterization of fully deacetylated chitosan. *International Journal of Biological Macromolecules*, *5*(1), 49–52.

Dutta, P. K., Tripathi, S., Mehrotra, G. K., & Dutta, J. (2009). Perspectives for chitosan based antimicrobial films in food applications. *Food Chemistry*, *114*(4), 1173–1182.

Epure, V., Griffon, M., Pollet, E., & Avérous, L. (2011). Structure and properties of glycerol-plasticized chitosan obtained by mechanical kneading. *Carbohydrate Polymers*, *83*(2), 947–952.

Favis, B. D., Rodriguez, F., & Ramsay, B. A. (2003). US patent no. 6,605,657 B1.

Favis, B. D., Rodriguez, F., & Ramsay, B. A. (2005). US patent no. 6,844,380 B2.

Favis, B. D., & Therrien, D. (1991). Factors influencing structure formation and phase size in an immiscible polymer blend of polycarbonate and polypropylene prepared by twin-screw extrusion. *Polymer*, *32*(8), 1474–1481.

Flaconneche, B., Martin, J., & Klopffer, M. H. (2001). Permeability, diffusion and solubility of gases in polyethylene, polyamide 11 and poly (vinylidene fluoride). *Oil & Gas Science and Technology—Revue de l'IFP*, *56*(3), 261–278.

Garlotta, D. (2001). A literature review of poly(lactic acid). *Journal of Polymers and the Environment*, *9*(2), 63–84.

Hernandez-Izquierdo, V. M., & Krochta, J. M. (2008). Thermoplastic processing of proteins for film formation—A review. *Journal of Food Science*, *73*(2), R30–R39.

Holmes, P. A. (1985). Applications of PHB—A microbially produced biodegradable thermoplastic. *Physics in Technology*, *16*(1), 32.

Kittur, F. S., Kumar, K. R., & Tharanathan, R. N. (1998). Functional packaging properties of chitosan films. *Zeitschrift für Lebensmitteluntersuchung und -Forschung A*, *206*(1), 44–47.

Kurek, M., Ščetar, M., Voilley, A., Galić, K., & Debeaufort, F. (2012). Barrier properties of chitosan coated polyethylene. *Journal of Membrane Science*, *403–404*(0), 162–168.

Leceta, I., Guerrero, P., & de la Caba, K. (2013). Functional properties of chitosan-based films. *Carbohydrate Polymers*, *93*(1), 339–346.

Leceta, I., Guerrero, P., Ibarburu, I., Dueñas, M. T., & de la Caba, K. (2013). Characterization and antimicrobial analysis of chitosan-based films. *Journal of Food Engineering*, *116*(4), 889–899.

Liu, H., Xie, F., Yu, L., Chen, L., & Li, L. (2009). Thermal processing of starch-based polymers. *Progress in Polymer Science*, *34*(12), 1348–1368.

Marić, M., & Macosko, C. W. (2001). Improving polymer blend dispersion in mini-mixers. *Polymer Engineering & Science*, *41*(1), 118–130.

Martínez-Camacho, A. P., Cortez-Rocha, M. O., Graciano-Verdugo, A. Z., Rodríguez-Félix, F., Castillo-Ortega, M. M., Burgos-Hernández, A., et al. (2013). Extruded films of blended chitosan, low density polyethylene and ethylene acrylic acid. *Carbohydrate Polymers*, *91*(2), 666–674.

Martino, V., Pollet, E., & Avérous, L. (2011). Novative biomaterials based on chitosan and poly(ε-caprolactone): Elaboration of porous structures. *Journal of Polymers and the Environment*, *19*(4), 819–826.

Matet, M., Heuzey, M.-C., & Ajji, A. (2014). Morphology and antibacterial properties of plasticized chitosan/metallocene polyethylene blends. *Journal of Materials Science*, *49*(15), 5427–5440.

Matet, M., Heuzey, M.-C., Pollet, E., Ajji, A., & Avérous, L. (2013). Innovative thermoplastic chitosan obtained by thermo-mechanical mixing with polyol plasticizers. *Carbohydrate Polymers*, *95*(1), 241–251.

McKeen, L. W. (2012a). *Introduction to permeation of plastics and elastomers permeability properties of plastics and elastomers* (3rd ed.). Amsterdam: Elsevier.

McKeen, L. W. (2012b). *Polyolefns, polyvinyls, and acrylics permeability properties of plastics and elastomers* (3rd ed.). Amsterdam: Elsevier.

Mekonnen, T., Mussone, P., Khalil, H., & Bressler, D. (2013). Progress in bio-based plastics and plasticizing modifications. *Journal of Materials Chemistry A*, *1*(43), 13379–13398 [10.1039/C3TA12555F].

Meng, Q., Heuzey, M.-C., & Carreau, P. J. (2014). Hierarchical structure and physicochemical properties of plasticized chitosan. *Biomacromolecules*, *15*(4), 1216–1224.

Mir, S., Yasin, T., Halley, P. J., Siddiqi, H. M., & Nicholson, T. (2011). Thermal, rheological, mechanical and morphological behavior of HDPE/chitosan blend. *Carbohydrate Polymers*, *83*(2), 414–421.

Namiki, M. (1988). Chemistry of Maillard reactions: Recent studies on the browning reaction mechanism and the development of antioxidants and mutagens. In C. O. Chichester, & B. S. Schweigert (Eds.), *Advances in food research* (32) (pp. 115–184). San Diego, California: Academic Press.

Quintana, R., Persenaire, O., Bonnaud, L., & Dubois, P. (2012). Recent advances in (reactive) melt processing of cellulose acetate and related biodegradable biocompositions. *Polymer Chemistry*, *3*(3), 591–595 [10.1039/C1PY00421B].

Ravi Kumar, M. N. V. (2000). A review of chitin and chitosan applications. *Reactive and Functional Polymers*, *46*(1), 1–27.

Rinaudo, M. (2006). Chitin and chitosan: Properties and applications. *Progress in Polymer Science*, *31*(7), 603–632.

Roberts, G. A. F. (1992). *Preparation of chitin and chitosan*. Indianapolis: Chitin Chemistry, The MacMillan Press Ltd, Indianapolis, p. 54–83.

Rodriguez-Gonzalez, F. J., Ramsay, B. A., & Favis, B. D. (2003). High performance LDPE/thermoplastic starch blends: A sustainable alternative to pure polyethylene. *Polymer*, *44*(5), 1517–1526.

Sears, J. K., & Darby, J. R. (1982). Mechanism of plasticizers action. In J. K. Sears, & J. R. Darby (Eds.), *The technology of plasticizers* (pp. 35–77). New York, NY: John Wiley and Sons.

Srinivasa, P. C., Ramesh, M. N., & Tharanathan, R. N. (2007). Effect of plasticizers and fatty acids on mechanical and permeability characteristics of chitosan films. *Food Hydrocolloids*, *21*(7), 1113–1122.

Suyatma, N. E., Tighzert, L., Copinet, A., & Coma, V. (2005). Effects of hydrophilic plasticizers on mechanical, thermal, and surface properties of chitosan films. *Journal of Agricultural and Food Chemistry*, *53*(10), 3950–3957.

Tanaka, M., Huang, J. R., Chiu, W. K., Ishizaki, S., & Taguchi, T. (1993). Effect of the maillard reaction on functional properties of chitosan. *Nippon Suisan Gakkaishi*, *59*(11), 1915–1921.

Zhang, H. Z., He, Z. C., Liu, G. H., & Qia, Y. Z. (2009). Properties of different chitosan/low-density polyethylene antibacterial plastics. *Journal of Applied Polymer Science*, *113*(3), 2018–2021.